

Current fluctuation spectra of liquid argon near its triple point

J. Bosse

Max-Planck-Institut für Physik und Astrophysik, 8 München, West Germany

W. Götze

Physik-Department der Technischen Universität München, 8046 Garching and Max-Planck-Institut für Physik und Astrophysik, 8 München, West Germany

M. Lücke*

Department of Physics, Harvard University, Cambridge, Massachusetts 02138

(Received 13 May 1977)

The mode-coupling theory for the dynamics of classical liquids formulated by the present authors has been applied to calculate the fluctuation spectra of the transverse and longitudinal currents, as well as the dynamical transport coefficients for liquid argon near its triple point. The results are compared with the neutron scattering data and with the molecular-dynamics calculations.

I. INTRODUCTION

In this paper, we report on the numerical results for the current correlation functions of liquid argon which were obtained from our mode-coupling theory for simple classical liquids.¹ Liquid argon is known as the representative example to check theories on liquids² since it has been studied extensively by neutron scattering experiments^{2,3} as well as by molecular-dynamics simulations.^{2,4,5}

In the calculations, we used as input data the number density $n = 2.14 \times 10^{22} \text{ cm}^{-3}$ the temperature $T = 85 \text{ }^\circ\text{K}$, the particle mass $m = 66.3 \times 10^{-24} \text{ g}$ and the Lennard-Jones potential $v(r)$ with parameters $\epsilon = 119.8 k_B \text{ }^\circ\text{K} = 165.37 \times 10^{-16} \text{ erg}$, $\sigma = 3.405 \text{ \AA}$ used by Rahman.⁴ The liquid structure factor $S(q)$ and the pair correlation function $g(r)$ were taken from the experiment reported by Yarnell *et al.*⁶ In evaluating integrals of products of $g(r)$ with second derivatives of the potential, we adopted the commonly accepted approximation

$$4\pi \frac{n}{m} r^2 g(r) v''(r) \approx 3\Omega_E^2 \delta(r - r_0). \quad (1)$$

For argon, the characteristic length parameter is $r_0 = 3.4 \text{ \AA}$ and the Einstein frequency is $\Omega_E = 0.74 \times 10^{13} \text{ sec}^{-1}$.⁷

The fluctuation spectrum of a dynamical variable A is defined by the Fourier transform of the time correlations $\langle \delta A^*(t) \delta A \rangle$ of the fluctuation $\delta A = A - \langle A \rangle$

$$\phi_A''(\omega) = \frac{1}{2} \int_{-\infty}^{+\infty} dt e^{it\omega} \frac{\langle \delta A^*(t) \delta A \rangle}{\langle \delta A^* \delta A \rangle}. \quad (2)$$

In scattering experiments, fluctuation spectra of certain dynamical variables are directly measured. The density fluctuation spectrum is obtained from (2) with A replaced by the particle density of wave

number q , $A = \rho(\vec{q})$. It yields Van Hove's scattering function

$$S(q, \omega) = \phi_{\rho(\vec{q})}''(\omega) S(q) / \pi, \quad (3)$$

which has been determined by neutron scattering.³ The fluctuation spectrum of the longitudinal current $\phi_L''(q, \omega)$ is also given by the density excitation spectrum via particle conservation

$$\phi_L''(q, \omega) = \frac{\omega^2}{\Omega_0^2(q)} \phi_{\rho(\vec{q})}''(\omega) \quad (4)$$

with

$$\Omega_0^2(q) = \frac{k_B T}{m} \frac{q^2}{S(q)}.$$

In addition to the spectra (3) and (4), molecular-dynamics calculations yield the spectrum of the transverse current $\phi_T''(q, \omega)$.^{4,5} It was also possible⁵ to determine the fluctuation spectra of the transverse and the longitudinal stresses, $D_{T,L}''(\omega)$. The latter quantities ought to be considered as dynamical transport coefficients; their zero-frequency limits determine the shear viscosity $\eta = nmD_T''(\omega=0)$ and the sound damping constant $\Gamma = \frac{4}{3}\eta + \xi = nmD_L''(\omega=0)$, respectively. The mode-coupling theory gives approximations for the quantities mentioned above.¹

For theoretical discussions, it is most convenient to introduce the Laplace transform of correlations

$$\phi_A(z) = \pm i \int_{-\infty}^{+\infty} dt \Theta(\pm t) e^{itz} \frac{\langle \delta A^*(t) \delta A \rangle}{\langle \delta A^* \delta A \rangle}, \quad \text{Im} z \geq 0. \quad (5)$$

These functions are analytic for nonreal frequencies z and they decrease at least like $1/z$ for large z . Functions $F(z)$ with such an analytic behavior are discontinuous at the real axis

$$F(\omega \pm i0) = F'(\omega) \pm iF''(\omega). \quad (6)$$

The spectral function $F''(\omega)$ determines $F(z)$ and $F'(\omega)$, in particular, according to

$$F(z) = \int_{-\infty}^{+\infty} \frac{d\omega}{\pi} \frac{F''(\omega)}{\omega - z}. \quad (7)$$

The spectral function corresponding to $\phi_A(z)$ is given by Eq. (2). The current correlation functions can be written in terms of generalized wave-number and frequency-dependent transport coefficients $D_{T,L}(q, z)$ ¹

$$\phi_T(q, z) = \frac{-1}{z + q^2 D_T(q, z)}, \quad (8a)$$

$$\phi_L(q, z) = \frac{-1}{z - \Omega_0^2(q)/z + q^2 D_L(q, z)}. \quad (8b)$$

Here $\Omega_0(q)$ is a characteristic low-frequency restoring force for density fluctuations which was defined in Eq. (4). Formulas (8) ensure the correct zeroth and second frequency moments for $S(q, \omega)$ and the correct zeroth frequency moment for the current correlations. $D_{T,L}(q, z)$ have a spectral representation (7); for $q=0$ they reduce to the dynamical transport coefficients mentioned before.¹ $D_{T,L}(q, z)$ can be expressed in terms of relaxation kernels $M_{T,L}(q, z)$:

$$q^2 D_T(q, z) = -\frac{\Omega_T^2(q)}{z + M_T(q, z)}, \quad (9a)$$

$$q^2 D_L(q, z) = -\frac{\Delta^2(q)}{z + M_L(q, z)}, \quad (9b)$$

where $\Delta^2(q) = \Omega_L^2(q) - \Omega_0^2(q)$, and $\Omega_{L,T}^2(q)$ are the well-known second frequency moments of the current fluctuation spectra given by the potential and $g(r)$.^{1,7} The correct fourth frequency moment of $S(q, \omega)$ is ensured by the representation (9b).

In addition to the free-particle contribution, the relaxation kernels include terms which reflect the damping of current fluctuations due to decay into pairs of current excitations.¹ There are two decay channels: decay into two longitudinal modes [contribution F_1, F_3 in Eqs. (51) of Ref. 1] and decay into one longitudinal and one transverse mode [contribution F_2 in Eq. (51) of Ref. 1]. The decay rates have to be calculated self-consistently with the fluctuation spectra $\phi_{T,L}''(q, \omega)$. Longitudinal and transverse excitations influence each other via the decay processes.

For later use, let us finally mention an exact expression for $S(q, \omega=0)$, a quantity which is needed for the interpretation of relaxation rates of NMR experiments, for example. Combining Eqs. (3), (9), and (7) we have

$$S(q, \omega=0) = \frac{1}{\pi} S(q) \left(\frac{\Omega_L^2(q)}{\Omega_0^2(q)} - 1 \right) / M_L''(q, \omega=0). \quad (10)$$

II. RESULTS

In Fig. 1, the relaxation spectra $M_{T,L}''(q, \omega)$ are shown for a series of representative values of q . The free-particle contribution is not important for momenta below 2 \AA^{-1} . However, for momenta exceeding 3 \AA^{-1} the free-particle contribution becomes essential. Our crude handling of this contribution to the current decay rates is expected to account for deviations from experiment. For large $q \geq 6 \text{ \AA}^{-1}$, however, the liquid motion is essentially

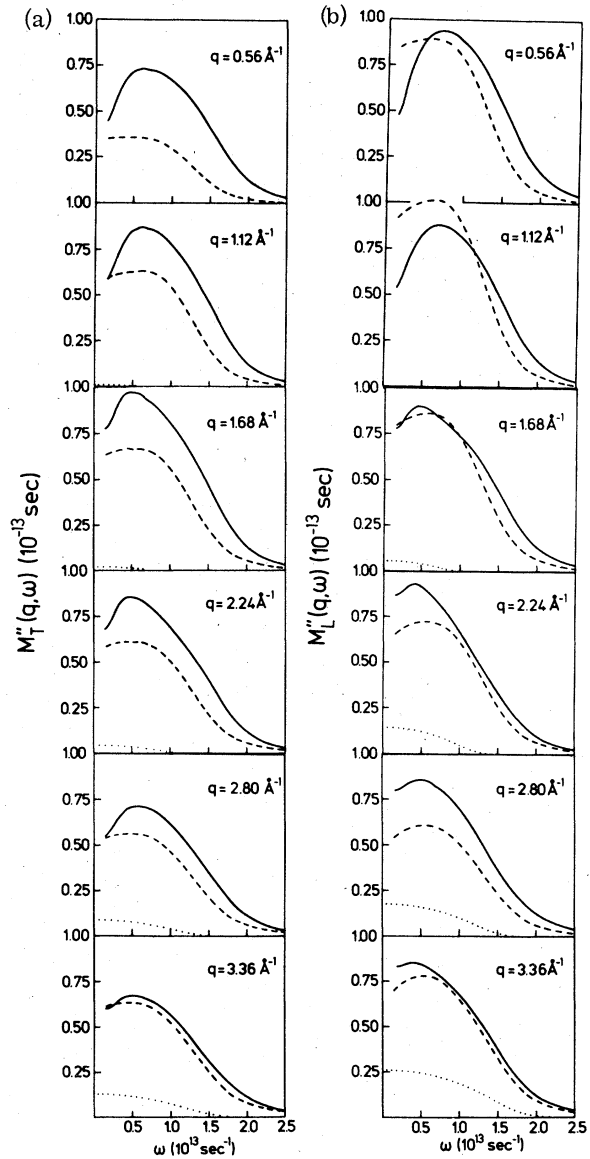


FIG. 1. Relaxation spectra for (a) transverse and (b) longitudinal current fluctuations (full curves) compared with the results of Ref. 8 (dashed curves). Free-particle contribution is indicated by the dotted curves.

free, mode-decay processes become unimportant, and the relaxation kernel [Eq. (55f) of Ref. 1] is exact.

In agreement with our earlier work,⁸ we find a sharp decrease of $M''(q, \omega)$ for frequencies larger than $1.5 \times 10^{13} \text{ sec}^{-1}$, since the energy of a two-mode excitation cannot exceed $2\Omega_E$ considerably. The introduction of other decay channels should add only a small and smooth background to our $M''(q, \omega)$; we therefore consider the cut-off at about $2\Omega_E$ in $M''(q, \omega)$ a realistic feature of liquid dynamics.

Over short distances, there is no remarkable

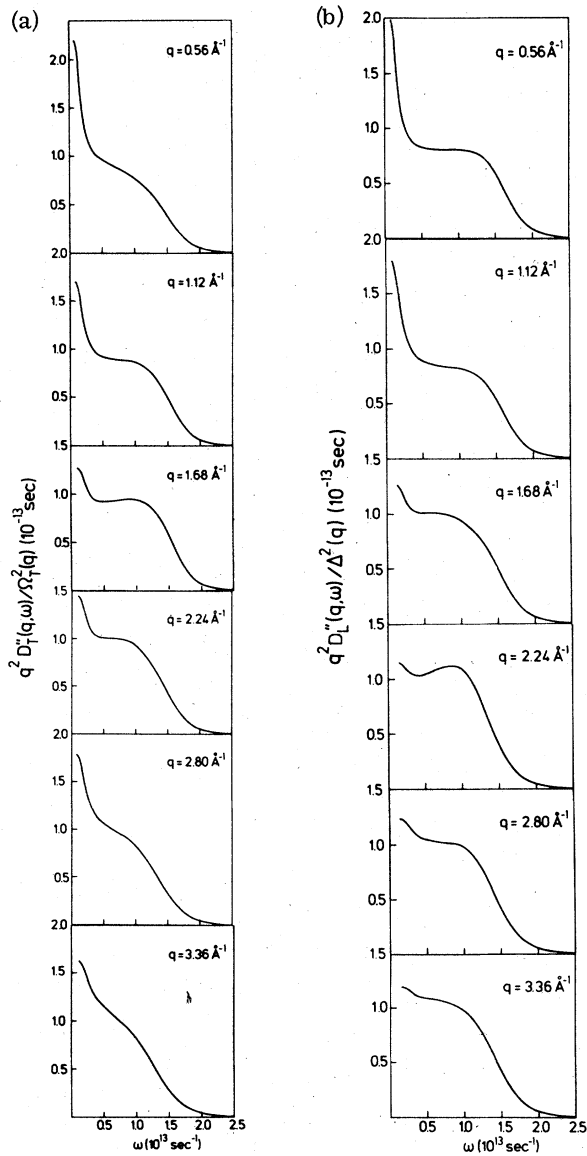


FIG. 2. Normalized coefficients (a) $q^2 D_T''(q, \omega) / \Omega_T^2(q)$ and (b) $q^2 D_L''(q, \omega) / \Delta^2(q)$ corresponding to the relaxation kernels given in Fig. 1.

difference between longitudinal and transverse particle motion. In particular, the mode-decay vertices¹ for a decay into a pair of longitudinal modes or into one longitudinal and one transverse mode do not differ appreciably for wave vectors q larger than, say, 1.5 \AA^{-1} . As a result, we find that for intermediate and large q , both decay channels contribute about equal amounts to the relaxation spectra. This feature is changed drastically, however, for small wave numbers. While the convolution integral of one longitudinal and one trans-

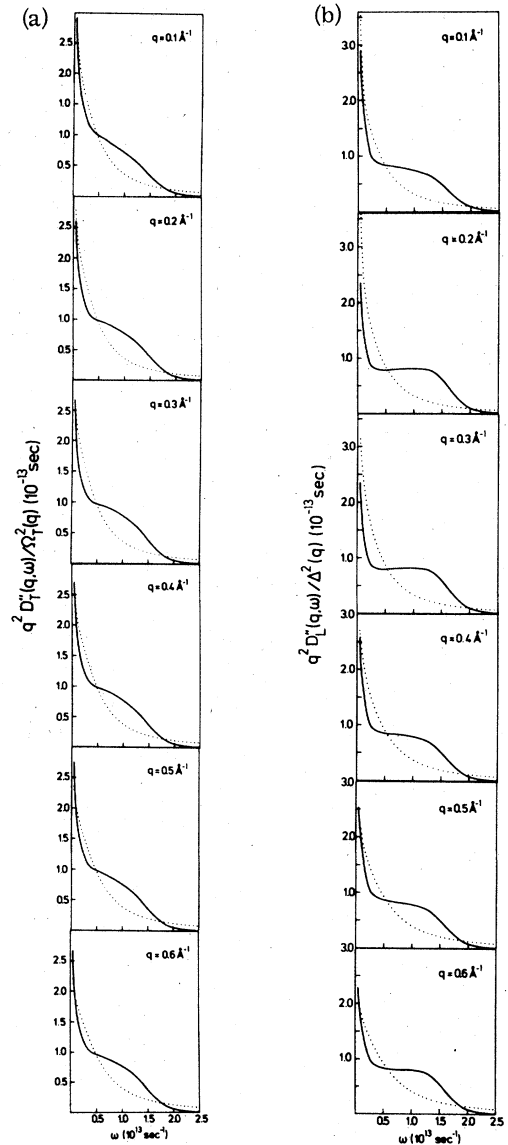


FIG. 3. Full curves show the coefficients (a) $q^2 D_T''(q, \omega) / \Omega_T^2(q)$ and (b) $q^2 D_L''(q, \omega) / \Delta^2(q)$ for small wave vectors ($q = 0.1 - 0.6 \text{ \AA}^{-1}$) in comparison with the molecular-dynamics results of Levesque, Verlet, and K urkjarvi (Ref. 5) (dotted curves; representing the fits given in Ref. 5).

verse mode [F_2 in Eq. (51b) of Ref. 1] yields a contribution to relaxation which decreases monotonically as a function of ω , the contributions due to decays into longitudinal modes [F_1 and F_3 in Eq. (51b) of Ref. 1] tend to cancel each other for $\omega \rightarrow 0$. Indeed, for $q=0$ and $\omega=0$ the decay into longitudinal modes is impossible [$L(k, \omega=0)=0$ in Eq. (74b) of Ref. 1]; for $q=0$ the decay into longitudinal modes contributes a term to the relaxation spectra which increases as $\omega^{1/2}$. This explains the low-frequency dip in $M''(q, \omega)$ which is the more pronounced the smaller q . The singular behavior of $M''(q=0; \omega)$ implies the well understood long-time anomaly² of $D''(q=0; \omega)$. Since the present theory ignores the low-frequency heat fluctuations, the value of $M''(q=0; \omega \rightarrow 0)$ is underestimated. Hence the long-time singularity seems to be overemphasized by our approximations. In our first version of the mode-coupling theory,⁸ the long-time anomaly has been treated incorrectly, since our crude treatment of the vertex implied a wrong long-wavelength asymptotics for $D(q, z)$.

In principle, relaxation spectra may be extracted from molecular-dynamics experiments. To do so, one evaluates $\phi_{T,L}(q, z)$ according to Eq. (7) using the experimental spectrum and then one solves Eqs. (8) and (9) for $M_{L,T}(q, z)$.⁸ This procedure is, however, most sensitive to small changes in $\phi''(q, \omega)$, which often result in big variations of $M''(q, \omega)$. We therefore consider such a comparison between theory and experiment not very reasonable.

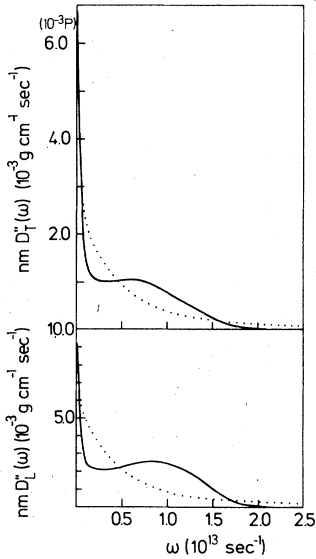


FIG. 4. Dynamical transport coefficients $D_T''(\omega)$ and $D_L''(\omega)$ as a function of ω (full curves) compared with the molecular-dynamics results of Levesque *et al.* (Ref. 5) (dotted curves; representing fits to MD results).

The behavior of the normalized coefficients $q^2 D_T''(q; \omega)/\Omega_T^2(q)$ and $q^2 D_L''(q, \omega)/\Delta^2(q)$ in Fig. 2 is implied by the properties of the relaxation kernels discussed above. These coefficients exhibit a resonance of width not larger than $0.2 \times 10^{13} \text{ sec}^{-1}$ due to long-time anomalies and a broad background with a sharp cutoff at about $2\Omega_p$. The central resonance is the more pronounced the smaller q . As a result $D_{T,L}''(q, \omega)$ look like superpositions of two resonances. In fact, Levesque *et al.*⁵ fitted

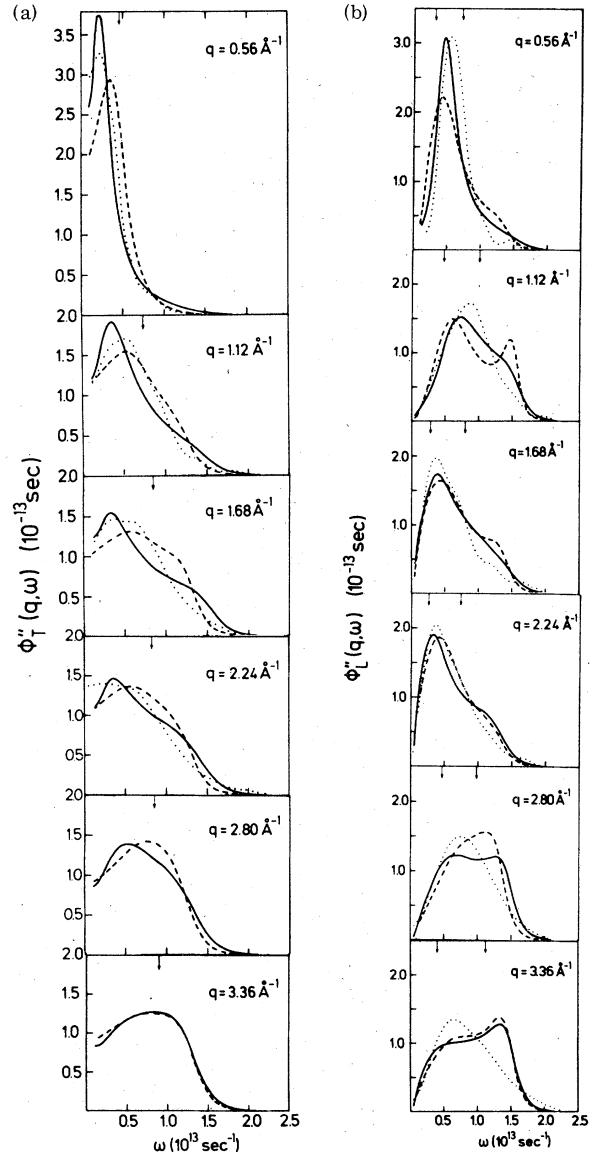


FIG. 5. Normalized fluctuation spectra for (a) transverse and (b) longitudinal currents (full curves). The dashed curves are the earlier results of Götze and Lücke (Ref. 8) and the dotted curves are Rahman's molecular dynamic calculations (Ref. 4). The small arrows indicate the values of $\Omega_T(q)$ in (a) and $\Omega_0(q)$ and $\Omega_L(q)$ in (b).

their data for the transverse current correlation functions by a superposition of two Lorentzians for $D_T''(q, \omega)$. In the longitudinal case, they found that no satisfactory fit could be achieved by using only one Lorentzian in addition to a heat diffusion term which was introduced explicitly in their fit⁵; thus, the longitudinal correlations were fitted by a superposition of three Lorentzians for $D_L''(q, \omega)$. In Fig. 3, their results are compared with the present theory. There is an overall agreement between theory and experiment, although the theoretical spectral functions exhibit a more pronounced structure than the experimental curves. The discrepancy between the present theory and the experimental results⁵ is also evident from Fig. 4, exhibiting the dynamical transport coefficients. Contrary to the experiment, we get a plateau in the spectrum for frequencies between 0.2 and 1.0 $\times 10^{13}$ sec⁻¹. We do not feel able to judge the rele-

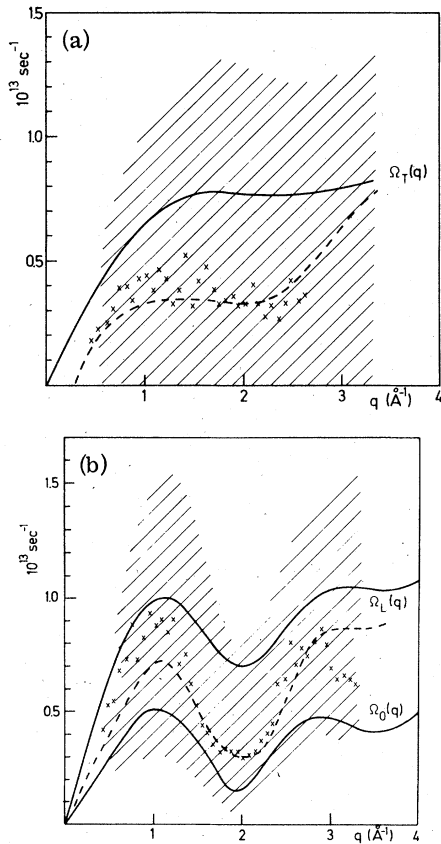


FIG. 6. The dashed curves represent the peak positions for the (a) transverse and (b) longitudinal current excitations in comparison with Rahman's data (Ref. 4) (crosses). Within the shaded area the spectrum drops to half of its maximum value. The full curves are the characteristic frequencies defined by the second moments $\Omega_{T,L}(q)$ and the inverse second moment $\Omega_0(q)$ of the spectra.

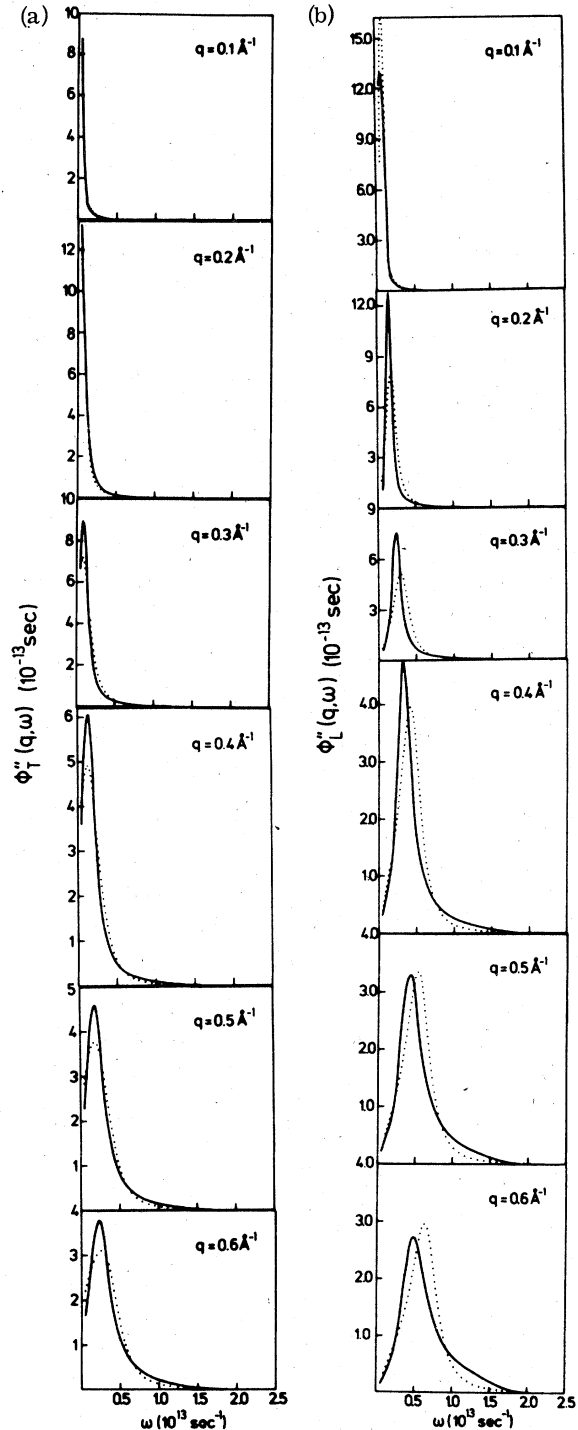


FIG. 7. Normalized long-wavelength excitation spectra for (a) transverse and (b) longitudinal currents (full curves) compared with Levesque *et al.* (Ref. 5) data [dotted curves, produced from Eqs. (8) using the fit parameters given in Ref. 5].

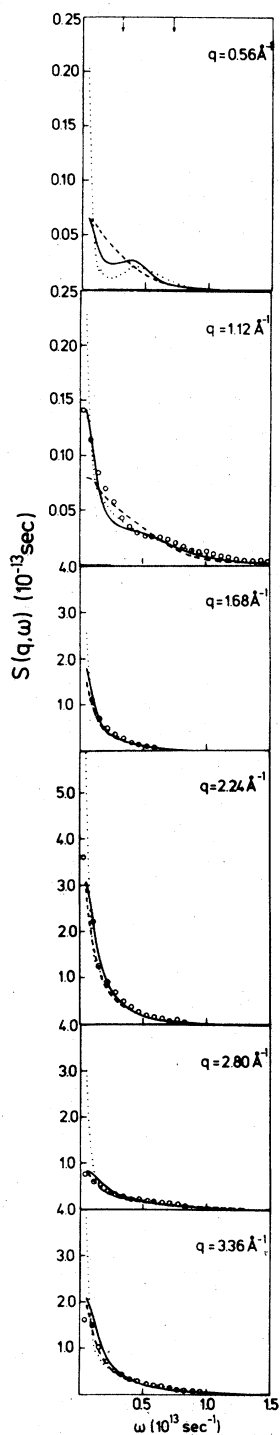


FIG. 8. Dynamical structure factor (full curves) in comparison with the neutron scattering cross sections of Sköld *et al.* (Ref. 3) (circles), Rahman's molecular dynamics results (Ref. 4) (dotted curves), and our previous calculations (Ref. 8) (dashed curves).

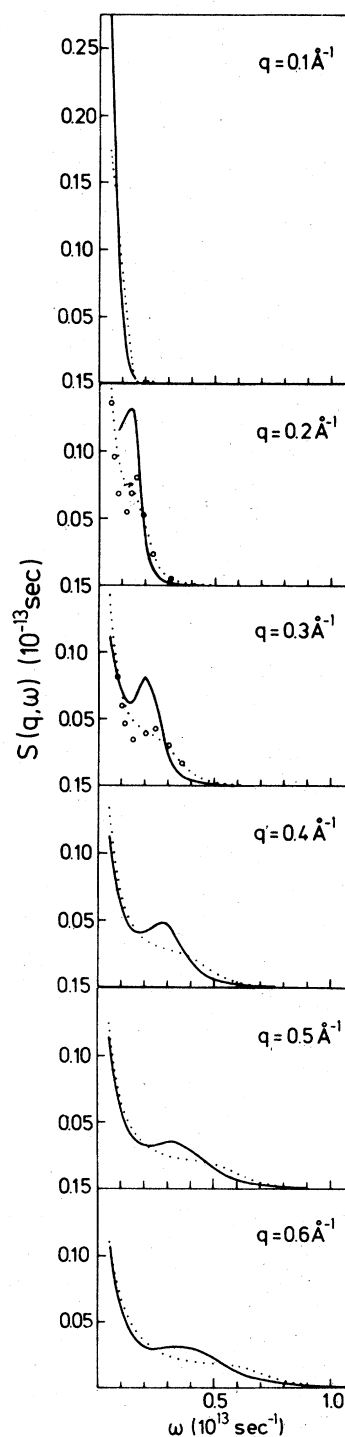


FIG. 9. Dynamical structure factor (full curves) compared with the molecular dynamics results (Ref. 5) of Levesque *et al.* (dotted curves, fit produced as in Fig. 7). For $q = 0.2 \text{ \AA}^{-1}$ and $q = 0.3 \text{ \AA}^{-1}$, we also indicated the actual MD results taken from Fig. 8 of Ref. 5 (circles).

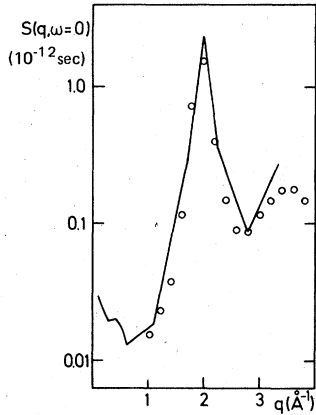


FIG. 10. $S(q, \omega=0)$ (full curve) compared with the neutron scattering data of Sköld *et al.* (Ref. 3) (circles).

vance of these discrepancies, since the uncertainties of the only existing very difficult experiment⁵ are unknown to us. Moreover, of course, the fit of the original data with two exponentials introduces artifacts for very high and for very low frequencies. Discrepancies between the fit and the molecular dynamics data due to the high-frequency Lorentzian tails have been reported in Ref. 5 for $q \geq 1 \text{ \AA}^{-1}$ already. On the other hand, for very low frequencies, it is well known that $D''(\omega) = D''(0) - \alpha\omega^{1/2}$, while the experiments are reported⁵ to be best fitted by a narrow regular Lorentzian.

The molecular-dynamics results for the transport coefficients given by Levesque *et al.*⁵ are $\eta_{LVK} = nmD_T''(\omega=0) = 3.64 \times 10^{-3} \text{ P}$ ($3.71 \times 10^{-3} \text{ P}$) and $\Gamma_{LVK} = nmD_L''(\omega=0) = 5.81 \times 10^{-3} \text{ P}$ ($7.10 \times 10^{-3} \text{ P}$) with $\xi_{LVK} = 0.26(0.58)$, where we added the ($q=0, \omega=0$) limits of the fitting curves in parentheses. For unknown reasons, these numbers differ from the transport coefficients found for liquid argon,⁹ $\eta_{\text{exp}} = 2.8 \times 10^{-3} \text{ P}$, and $\Gamma_{\text{exp}} = 6.0 \times 10^{-3} \text{ P}$ with $\xi_{\text{exp}}/\eta_{\text{exp}} = 0.8$. The correct $\omega^{1/2}$ extrapolation of the Levesque *et al.*⁵ data yields even larger values for the transport coefficients $\eta'_{LVK} = 4.7 \times 10^{-3} \text{ P}$ and $\Gamma'_{LVK} = 9.8 \times 10^{-3} \text{ P}$ with $\xi'/\eta' = 0.74$.

The present theory leads to still larger values of the transport coefficients [Sec. 4 of Ref. 1]: $\eta = 6.9 \times 10^{-3} \text{ P}$ and $\Gamma = 32.7 \times 10^{-3} \text{ P}$ with $\xi/\eta = 3.4$. These numbers were calculated from Eqs. (74)–(76) of Ref. 1 using $c_T = (\Omega_T(q)/q)_{q=0} = 853 \text{ msec}^{-1}$, $c_L = (\Omega_L(q)/q)_{q=0} = 1478 \text{ msec}^{-1}$, and $c_{th} = (\Omega_0(q)/q)_{q=0} = 595 \text{ msec}^{-1}$. The latter velocities were calculated according to Eqs. (26) and (41) of Ref. 1 using the $g(r)$ data of Yarnell *et al.*⁶ By plotting $[D_T''(\omega) - D_T''(\omega=0)]^2$ against ω we found a straight line for $\omega \leq 0.1 \times 10^{13} \text{ sec}^{-1}$ showing that the central peak in the dynamical transport coefficient $D_T''(\omega)$ caused by the long-time anomalies obeys the expected

$\omega^{1/2}$ law for frequencies up to $\omega_{SQ}^T \approx 10 \text{ psec}^{-1}$. In the longitudinal case, we can only conclude $\omega_{SQ}^L \lesssim 5 \text{ psec}^{-1}$, since $D''(\omega)$ was calculated in steps of $\Delta\omega = 0.05 \times 10^{13} \text{ sec}^{-1}$ prohibiting a more precise statement. Clearly, the present theory overemphasizes the low frequency resonance, since damping mechanisms due to decay into heat fluctuations have been neglected. This is also reflected by the large value of ξ/η , which according to Eq. (78) of Ref. 1 is not influenced by any approximations made in the calculation of the decay vertices.

In Fig. 5, the results for the current fluctuation spectra are compared with Rahman's data⁴ and with our earlier calculations.⁸ For large momenta ($q = 2.8 \text{ \AA}^{-1}$ and $q = 3.36 \text{ \AA}^{-1}$), there are systematic deviations between theory and experiment, presumably due to our rough treatment of the free particle motion. Otherwise we consider the agreement between theory and experiment satisfactory. The earlier results for the long-wavelength fluctuations have been improved. An overall characterization of the liquid excitations is given in Fig. 6 where the resonance peak positions and widths are shown together with the characteristic liquid frequencies $\Omega_0(q)$ and $\Omega_{L,T}(q)$. Notice that in agreement with experiment we find that transverse excitation peaks cease to exist for wave numbers smaller than about 0.3 \AA^{-1} . The long-wavelength current fluctuation spectra agree satisfactorily with the results of Levesque *et al.*⁵ as is demonstrated in Fig. 7. In Fig. 8, Van Hove's dynamical structure factor is compared with Rahman's data⁴ as well as the neutron scattering cross sections of Sköld *et al.*³ This set of figures is the least sensitive one for a comparison of theory and experiment. Notice that the present theory exhibits a side peak of $S(q, \omega)$ for $q = 0.56 \text{ \AA}^{-1}$ in qualitative agreement with Rahman's data. This side peak is a consequence of the cutoff at about $2\Omega_E$ in our $M_L''(q, \omega)$. If the frequency dependence of $M''(q, \omega)$ is ignored, which is often done in phenomenological discussions,⁷ this interesting detail will be missing. In Fig. 9, the long-wavelength structure factor is compared with the molecular dynamics results of Levesque *et al.*⁵ Contrary to Rahman,⁴ no side peak of $S(q, \omega)$ for $q \approx 0.5 \text{ \AA}^{-1}$ is reported by Levesque *et al.*; their curve indicates only a slight shoulder. The reason for this inconsistency of the two existing MD results is not known to us. Nevertheless, we would conclude from Fig. 9 that the present theory overemphasizes the side-peaks, which is presumably caused by ignoring heat fluctuations.

Finally, in Fig. 10, $S(q, \omega=0)$ is compared with neutron scattering data of Sköld *et al.*³ The quantitative discrepancies between theory and experi-

ment reflect our overestimating the long time anomalies in $D_L''(q, \omega)$, which is equivalent to underestimating $M_L''(q, \omega=0)$. According to (10) this leads to larger values for $S(q, \omega=0)$.

Taking into account that the mode coupling theory^{1,8} is the first attempt to calculate current fluctuation spectra for a realistic classical liquid using neither phenomenological assumptions on the relaxation kernels nor fit parameters, we con-

sider the comparison between our results and experimental data encouraging. For improvements of this theory, it would be extremely helpful to have experimental or other theoretical information on static and dynamic energy fluctuations as well as on the coupling of energy fluctuations with density fluctuations. Another bottleneck for improvements is the present-day ignorance of static three and four particle correlations in liquids.

*Deutsche Forschungsgemeinschaft fellow on leave from Physikdepartment der Technischen Universität München. Research supported in part by the National Science Foundation, under Grant DMR72-02977 A03.

¹J. Bosse, W. Götze, and M. Lücke, *Phys. Rev. A* **17**, 434 (1978), preceding paper.

²For a list of references the reader is referred to Ref. 1.

³K. Sköld, J. M. Rowe, G. Ostrowski, and P. D. Randolph, *Phys. Rev. A* **6**, 1107 (1972).

⁴A. Rahman, *Phys. Rev. Lett.* **19**, 420 (1967); *Neutron Inelastic Scattering* (International Atomic Energy

Agency, Vienna, 1968), p. 561.

⁵D. Levesque, L. Verlet, and J. Kurkijärvi, *Phys. Rev. A* **7**, 1690 (1973).

⁶J. L. Yarnell, M. J. Katz, and R. G. Wenzel, *Phys. Rev. A* **7**, 2130 (1973).

⁷Compare the discussion in the review article: J. R. D. Copley and S. W. Lovesey, *Rep. Prog. Phys.* **38**, 461 (1975).

⁸W. Götze and M. Lücke, *Phys. Rev. A* **11**, 2173 (1975).

⁹D. G. Naugle, J. H. Lunsford, J. R. Singer, *J. Chem. Phys.* **45**, 4669 (1966).